Engineering Structures 152 (2017) 819–831

Contents lists available at ScienceDirect

Engineering Structures

journal homepage: www.elsevier.com/locate/engstruct

Control of relative vibration between flexible appendages using passive and semi-active isolation

Hernán Garrido, Oscar Curadelli *, Daniel Ambrosini

National University of Cuyo, CONICET, Eng. Faculty, Mendoza, Argentina

ARTICLE INFO

Article history:
Received 12 June 2017
Revised 22 August 2017
Accepted 27 September 2017

Keywords:
Relative vibration
Differential vibration
Semi-active control
Ground-hook
Sky-hook

ABSTRACT

Relative vibration between two flexible subsystems can be detrimental to the performance of many engineering applications, such as optics-based instruments, machine tools, or adjacent industrial structures sharing piping. For the purpose of controlling this particular vibration, this paper presents two control approaches based on the passive and semi-active isolation at each subsystem: the *indirect* control *method*, consisting in the reduction of the individual vibration of each subsystem, and the *direct* control *method*, which aims to reduce the relative vibration between both subsystems. Necessary conditions for the feasibility of the *direct* control method are found, thereby reducing the universe of possible design configurations. From the traditional ground-hook and sky-hook control laws, which simulate, respectively, a damper between the body to be controlled and the support or the reference framework, it is generalized a control law called body-hook-body, which simulates a damper between both bodies to be controlled. Taking into account the performance and cost/complexity of the whole system, different alternatives for each vibration control method are numerically and experimentally studied. From the results, it is inferred that the proposed direct control method, using body-hook-body, is as effective as the traditional *indirect* control method, using ground-hook or sky-hook, but with lower cost and complexity.

1. Introduction

In some engineering applications, the relative vibration between points of a structure (or structures) is more problematic than the individual vibrations of such points; especially if the relative vibration cannot be reduced through a linking damping element due to architectural considerations [1] or physical constraints [2]. This particular problem is typical of multi-element antennas and in many optical arrangements or instruments such as telescopes, cameras, etc. For example, camera-in-hand robotic systems [3] are affected by the relative vibration between the camera and the target [4]. A distortion in the relative positions of optical elements of a telescope cause aberrations such as wave front error or defocusing [5–7]. Relative vibration between Automatic Optical Inspection (AOI) devices and the associated workpieces is critical in the inspection throughput [8]. In particle colliders [9] and interferometers [10], relative very small vibrations may result critical. The performance of machine tools is highly affected by the vibration of subsystems because affects the quality and precision of the machining [11,12]. On the other hand, in civil and industrial facilities, vibration in adjacent structures can cause pounding [13,14] or damage in piping connections [15].

In order to reduce vibrations, many control system have been proposed and are generally classified into passive [1], active [16], or semi-active [17–20]; although hybrid combinations are also common [21]. In a semi-active vibration control system, the properties of a passive device (e.g., a viscous damper) are conveniently adjusted in real-time by a controller through an auxiliary actuator (e.g., a valve) [22]. These systems are attractive because they offer the reliability, stability and simplicity of passive systems; while approaching the adaptability and performance of active systems with lower power demand [17].

Despite the large amount of available vibration control methods, there are only a few papers addressing the control of relative vibrations in general terms and explicitly [11,12]. This is attributable to the fact that *relative vibration* is commonly controlled, in an *indirect* way, by implementing systems that reduce the *individual vibrations* of each subsystem; e.g. by using an isolator at the vibration source [6] or isolators at the payloads [16,23]. Alternatively, when higher performance is required, active systems can be designed to control relative vibration in a *direct* way [8,10]; i.e. by formulating the control objective as the minimization of a specific relative vibration.

* Corresponding author at: Facultad de Ingeniería, Centro Universitario, Parque Gral. San Martín, (5500) Mendoza, Argentina.
E-mail address: ocuradelli@fing.uncu.edu.ar (O. Curadelli).

https://doi.org/10.1016/j.engstruct.2017.09.056
0141-0296/

Performance of semi-active control systems tends to that of active ones, mainly because both of them can use information sensed in points other than those in which control forces are exerted. This setup, which is usually referred to as non-collocated control [16,21,24], has shown to be effective in mitigating relative displacement, in a *direct* way, by using a properly-tuned semi-active controller [25,26]. However, these types of controller are model-based and consider full-state feedback, requiring a large number of sensors or a state observer [16]. On the other hand, controllers based on *sky-hook* [22] and *ground-hook* [27] control laws are easier to implement since they are model-free and only 2 variables have to be sensed [18]. Moreover, they are non-collocated control laws that can control individual vibrations very effectively.

This paper presents a simplified framework for the problem of relative vibrations mitigation, based on passive and semi-active isolation systems, using two approaches: an *indirect* control method that aims to reduce the relative vibrations, by reducing the individual vibrations; and a *direct* control method that aims to reduce relative vibrations, without necessarily reducing individual vibrations. While the *indirect* control method can be implemented with state-of-the-practice tools, the ability and technical advantages of semi-active control to reduce relative vibrations between structures has not been studied previously.

For the *direct* control method, necessary conditions of *feasibility* are found from a simplified model of the system response. This method is implemented through a simple control law called *body-hook-body*, obtained by the generalization of the *sky-hook* and *ground-hook* control laws widely known. To validate the new concept, an experimental and numerical comparative study on the performances of feasible semi-active realizations of the *direct* and *indirect* control methods is conducted.

From the results, it is concluded that the *direct* control method has practically the same performance in controlling relative vibrations as the *indirect* control method but with more versatility and less hardware complexity.

2. A brief theory of relative-vibration control

A simplified theoretical framework on relative vibration mitigation based on passive and semi-active control systems is presented in this section.

2.1. Problem statement

Consider the structure illustrated in Fig.1, which is comprised of two uncoupled flexible appendages that share the same support and can be modelled by a 2-degrees-of-freedom (DOFs) system. The *individual* displacements, measured with respect to an inertial reference frame, are denoted as $d_1(t)$ and $d_2(t)$; where t is the time.

Assuming that the excitation is induced by broad-band acceleration $\ddot{d}_g(t)$ at the structure support, the structural damping is low, and the response of each DOF (located at the payloads) is dominated by a single vibration mode of the corresponding appendage, the displacements of each DOF, measured with respect to the support, have the following approximate solutions [28]:

$$d_{1g}(t) = d_1(t) - d_g(t) = A_1 \sin(2\pi f_1 t + \theta_1), \tag{1}$$

$$d_{2g}(t) = d_2(t) - d_g(t) = A_2 \sin(2\pi f_2 t + \theta_2), \tag{2}$$

where $d_1(t)$, $d_2(t)$, $d_g(t)$ are the *absolute displacements* of each DOF and support respectively; A_1 and A_2 are amplitudes that depend on the excitation and the properties of the system (damping ratio, mass and static stiffness); f_1 and f_2 are frequencies that, in the uncontrolled case, are equal to the natural frequencies of the appendages f_{s1} and f_{s2}; and θ_1 and θ_2 are offset phases. The arguments of the sine functions, $2\pi f_1 t + \theta_1$ and $2\pi f_2 t + \theta_2$, are the instantaneous phases.

By convention in this paper, d_1, d_2, d_{1g} and d_{2g} are all referred to as *individual displacements*. The *relative displacement* $d_r(t)$ between both DOFs is the difference between Eqs. (1) and (2), which can be recast as follows:

$$\begin{aligned} d_r(t) &= d_{1g}(t) - d_{2g}(t) = d_1(t) - d_2(t) \\ &= 2A_1 \sin\left(\frac{2\pi\Delta_f t + \Delta_\theta}{2}\right) \cos\left(\frac{2\pi\Sigma_f t + \Sigma_\theta}{2}\right) \\ &\quad + \Delta_A \sin(2\pi f_2 t + \theta_2) \end{aligned} \tag{3}$$

where $\Delta_f = f_1 - f_2$, $\Delta_\theta = \theta_1 - \theta_2$, $\Delta_A = A_1 - A_2$, $\Sigma_f = f_1 + f_2$ and $\Sigma_\theta = \theta_1 + \theta_2$.

2.2. Control methods

From Eq. (3), two main control methods can be devised to attain the objective of reducing $d_r(t)$ (denoted as $\min|d_r|$ for briefness):

(1) *indirect* control method, classical approach, which seeks to control the relative vibrations through the reduction of individual vibrations, i.e. $\min|d_1|$ and $\min|d_2|$ or, alternatively, $\min|d_{1g}|$ and $\min|d_{2g}|$;
(2) *direct* control method, proposed in the present paper, which seeks to reduce the relative motion without necessarily reducing individual vibrations, i.e. $\min|d_1 - d_2|$ or, alternatively, $\min|d_{1g} - d_{2g}|$.

Tools for feasible implementation of the *indirect* control method are well-known [16,18,29]. For example, the objectives $\min|d_1|$ and $\min|d_2|$ can be reached by implementing, in each end of the appendages, 2 independent passive isolators or 2 semi-active isolators under the *sky-hook* control law. On the other hand, the

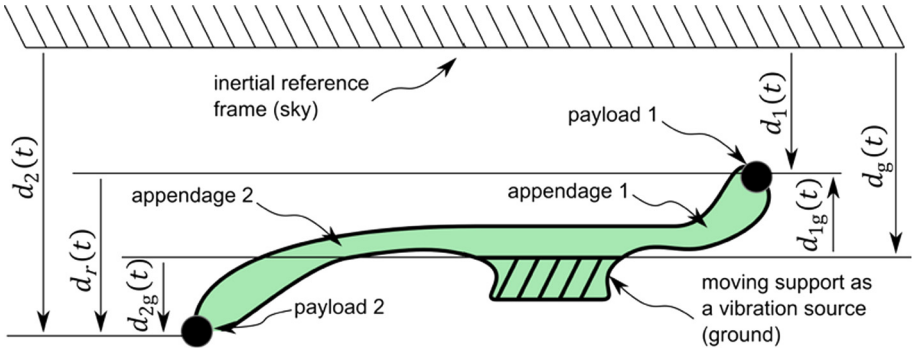

Fig. 1. A general structure with two flexible appendages.

alternative objectives $\min|d_1|$ and $\min|d_2|$ can be implemented using 2 passive dampers (if physically possible) or 2 semi-active isolators under the *ground-hook* control law.

In this paper, an implementation, method or alternative for controlling vibration is said to be "unfeasible" if bad performance can be predicted a priori without previous studies.

In order to implement a feasible *direct* control method where $A_1 \not\approx 0$, the following three necessary conditions are derived from the right-hand side of Eq. (3):

$$\Delta_\theta \approx 0 \tag{4}$$

$$\Delta_f \approx 0 \tag{5}$$

$$\Delta_A \approx 0 \tag{6}$$

Regarding condition (4), offset-phases difference, Δ_θ, is a constant that depends on the spatial influence of excitation on the appendages, such as e.g. when the appendages move in counter-phase due to a support rotation: $\Delta_\theta = \pi$ rad. Therefore, condition (4) is useful to determine whether the *direct* control method is unfeasible and discard it early as in the example given.

Neglecting the appendage masses with respect to payload masses, condition (5) can be satisfied by providing passive isolators on one or both appendages, thus reducing the natural frequencies from those of the appendages ($f_j = f_{sj}$) to those of the passively-isolated subsystems ($f_j = f_{pisj}$) aiming to tuning them. Another alternative would be replacing passive isolators by semi-active isolators with increasable effective damping in which the frequencies f_j can be finely adjusted automatically during operation between f_{minj} and f_{maxj}; where $f_{pisj} \leqslant f_{minj} \leqslant f_j \leqslant f_{maxj} \leqslant f_{sj}$.

For example, assuming that $f_{s1} < f_{s2}$, there are only two feasible passive-control alternatives using the *direct* control method: (1) providing the appendage 2 with a passive isolator such that $f_{s1} = f_{pis2}$ or (2) providing both appendages with passive isolators such that $f_{pis1} = f_{pis2}$. On the other hand, there are only three feasible semi-active control alternatives using the *direct* control method: (1) providing appendage 2 with a semi-active isolator such that $f_{min2} \leqslant f_{s1} \leqslant f_{max2}$; (2) providing appendage 1 with a semi-active isolator and appendage 2 with a passive isolator such that $f_{min1} \leqslant f_{pis2} \leqslant f_{max1}$; and (3) providing both appendages with semi-active isolators such that $[f_{min1}, f_{max1}] \cap [f_{min2}, f_{max2}] \neq \varnothing$.

It is interesting to note that, if $|\Delta_f|$ is small but not identically equal to zero ($\Delta_f \approx 0$), as expected in practice, the first term of Eq. (3) will eventually increase after a long time; i.e. phase-shift cumulates ($\pi\Delta_f t$). Hence, direct control method using passive control is feasible only for intermittent vibrations significantly shorter than $(2\Delta_f)^{-1}$; since f_1 and f_2 are constant over time. In contrast, semi-active control can compensate cumulative phase-shift; since it enables Δ_f to change sign in real time by tuning f_1 and/or f_2.The closeness between frequencies might be estimated by their absolute difference normalized with respect to their average ($\frac{2|\Delta_f|}{\Sigma_f}$). This is a representative figure because the normalized correlation between sine functions having the same amplitude and offset phase but different frequency is monotonically decreasing with $\frac{2|\Delta_f|}{\Sigma_f}$ if $\frac{2|\Delta_f|}{\Sigma_f} \leqslant 50\%$, as shown in Appendix A.

Finally, a priori, no general conclusion can be made for condition (6) since vibration amplitudes depend on several parameters.

The usefulness of these three necessary conditions is that any implementation case, in which one or more of such conditions are not satisfied, it is expected to be ineffective (*unfeasibility*) and, therefore, can be discarded a priori.

These results, valid for the structure previously presented, are generalizable to two n-DOF structures through modal decomposition. Namely, a set of three necessary conditions is obtained for each pair of vibration modes.

3. Control laws

Since their introduction in the 1970 s [22], sky-hook and ground-hook semi-active control laws have been broadly studied and applied [18,27,30,31]. In the present section, these control laws are first briefly revisited and then generalized under a new concept called *body-hook-body*.

As illustrated in Fig. 2(a), ground-hook simulates a "hook" between the body to be controlled and the "ground", where "ground" is actually the possibly-moving structure support (e.g., a building foundation, vehicle wheels or a satellite central hub). Similarly, sky-hook simulates a "hook" between the body to be controlled and the "sky", where "sky" is actually an inertial reference frame. [1]

In both control laws, the control force is effectively exerted by a vibrating *near body* (part of the structure, as shown in Fig. 2(a); or an auxiliary mass, as in semi-active tuned mass dampers [27,31,32]) that pulls or pushes adequately the *body to be controlled* through a variable damper [18,27,31,33]. This is done by adjusting its damping force (see Fig. 2b) through its characteristic (e.g. damping coefficient or normal force) according to the following expression:

$$F(\dot{x}_{RD}) = \begin{cases} F_{max}(\dot{x}_{RD}), & \dot{x}_C\dot{x}_{RD} > 0 \\ F_{min}(\dot{x}_{RD}), & \dot{x}_C\dot{x}_{RD} \leqslant 0 \end{cases} \tag{7}$$

in which: $\dot{x}_{RD}$ is the relative velocity between ends of the variable damper; $\dot{x}_C$ is the velocity of generalized coordinate to be controlled, as shown in Fig. 2(a). Displacement-based [31] and acceleration-based [30] versions replace $\dot{x}_C$ with x_C or $\ddot{x}_C$, respectively.

As shown in Fig. 2(a), the only difference between both control laws is the reference from which $\dot{x}_C$ is measured. Therefore, in order to control the relative vibration between two DOFs by means of the *direct* control method, it is proposed a simple control law called *body-hook-body* where $\dot{x}_C$ is defined between those DOFs. Thus, Eq. (7) defines the force for the *generalized body-hook-body* control law which has three particular cases depending on the definition of $\dot{x}_C$: (1) *ground-hook*, (2) *sky-hook*, and (3) *body-hook-body* (Fig. 2(a)).

Although, as with ground-hook and sky-hook [22] the effectiveness of body-hook-body must be assessed through simulations and/or experiments, conditions stated in Section 2.2 can be assessed to discard, a priori, unfeasible implementation cases.

4. Experimental setup and instrumentation

As a proof-of-concept, an experimental setup is proposed to compare the control alternatives which spring up from the concepts outlined in Sections 2 and 3. It is considered a structural typology frequent in artificial satellites that consists of a central rigid hub with long flexible appendages [34–37]. Commonly, the payloads of these space structures are devices whose performance can be affected by relative vibration between them (e.g., [10,16]).

Fig. 3(a) shows a panoramic view of the experimental setup, which comprises the following elements: two steel cantilever beams representing the flexible appendages; a shaking-table representing the supporting rigid hub (i.e., the "ground"); two pairs of masses as payloads; an isolator between the end of each appendage and its respective payload (see detailed view in Fig. 4); a

[1] Such emulated hook dampers can be quantified numerically in an average sense [40].

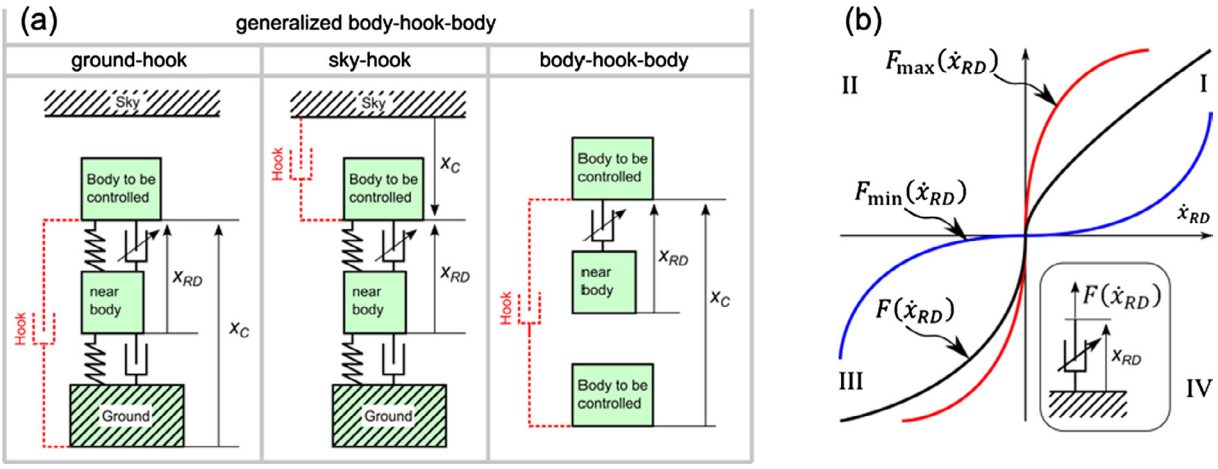

Fig. 2. (a) Ground-hook, sky-hook and body-hook-body control laws. (b) Variable damper model.

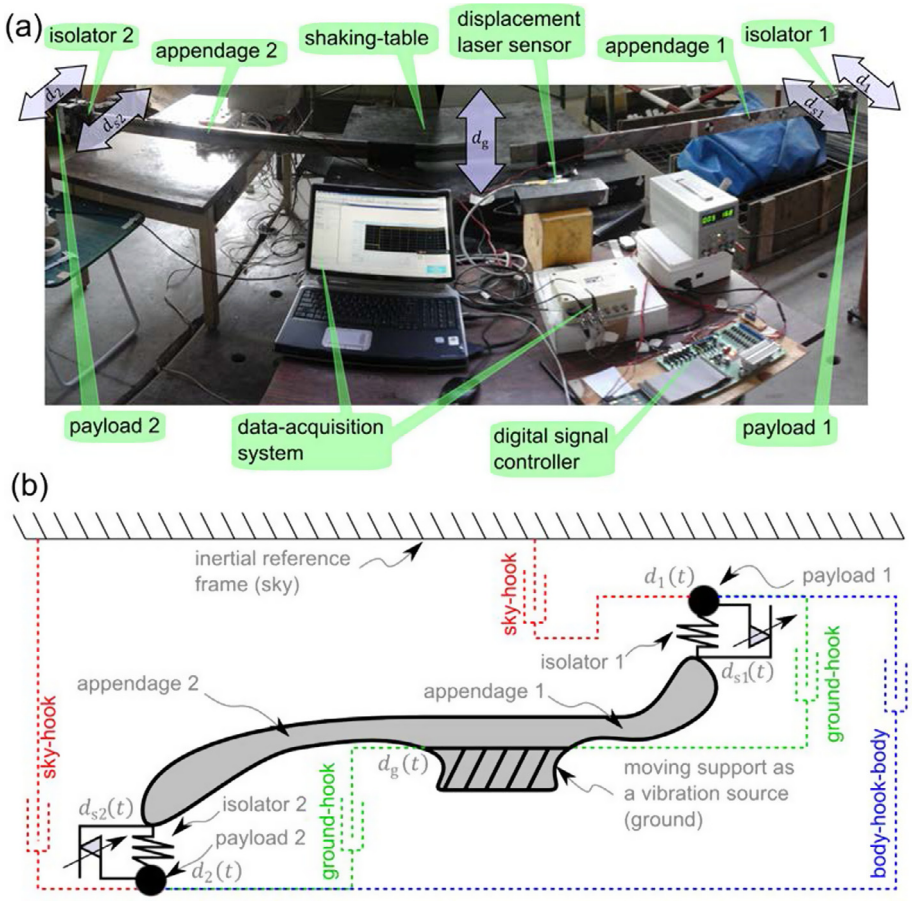

Fig. 3. (a) Panoramic view of the experimental setup. (b) Schematic diagram.

data-acquisition system to record displacements; a digital signal controller; and three laser sensors for control and evaluation purposes, one measuring the displacement of the support (d_g) and two measuring the individual displacements of the payloads (d_1 and d_2), all of them with respect to an inertial reference frame (i.e., the "sky"). Although, in real-life applications, the measurement of absolute displacement can be difficult, absolute-velocity and -acceleration can be easily measured for control purposes by means of inertial sensors.

For its part, Fig. 3(b) represents the structure, isolators, and payloads, in a simplified form. Besides, possible semi-active control laws are symbolized as 'hooks' in dashed lines.

Fig. 4 shows a detailed view of one of the isolators (both are identical). This device isolates in the horizontal direction the payload displacement (d_1 or d_2) from the appendage displacement (d_{s1} or d_{s2}) by using linear bearings. Two springs provide a restoring force, whereas damping is caused by two sources of friction: (1) the bearings and (2) a variable-friction damper consisting of

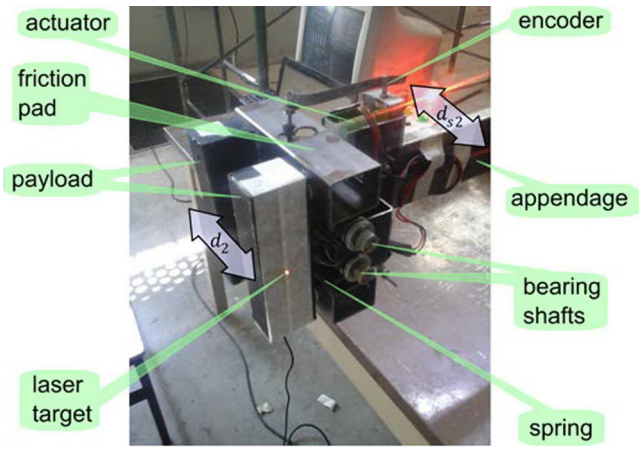

Fig. 4. Detailed view of an isolator placed between appendage and payload.

friction pads whose variable normal force is exerted by electromagnetic actuators. Besides for control purposes, analog encoders measure the relative displacements between the payloads and the respective appendage ends; i.e., $x_{RD1} = d_1 - d_{s1}$ and $x_{RD2} = d_2 - d_{s2}$. Velocities are calculated by the digital signal controller through the two-point finite difference method with a time step of 10 ms.

The described isolator has three modes of operation: (1) as a passive isolator, de-energizing the actuators; (2) as a semi-active isolator, driving the actuators in real-time; or (3) as a locking joint, blocking the isolation by means of a fixing plate and applying the maximum normal force.

5. Mathematical model

Assuming that each appendage can be modelled by a 1-DOF linear system and using the Coulomb model for the isolator friction forces, the whole mechanical system can be represented by the following nonlinear equations of motion (see Fig. 3(b)):

$$m_1\ddot{d}_1(t) + (F_{f1} + \mu N_1)\text{sign}(\dot{d}_1(t) - \dot{d}_{s1}(t)) + k_1(d_1(t) - d_{s1}(t)) = 0 \tag{8}$$

$$m_{s1}\ddot{d}_{s1}(t) + (F_{f1} + \mu N_1)\text{sign}(\dot{d}_{s1}(t) - \dot{d}_1(t)) + c_{s1}\dot{d}_{s1}(t) + k_1(d_{s1}(t) - d_1(t)) + k_{s1}d_{s1}(t) = k_{s1}d_g(t) + c_{s1}\dot{d}_g(t) \tag{9}$$

$$m_2\ddot{d}_2(t) + (F_{f2} + \mu N_2)\text{sign}(\dot{d}_2(t) - \dot{d}_{s2}(t)) + k_2(d_2(t) - d_{s2}(t)) = 0 \tag{10}$$

$$m_{s2}\ddot{d}_{s2}(t) + (F_{f2} + \mu N_2)\text{sign}(\dot{d}_{s2}(t) - \dot{d}_2(t)) + c_{s2}\dot{d}_{s2}(t) + k_2(d_{s2}(t) - d_2(t)) + k_{s2}d_{s2}(t) = k_{s2}d_g(t) + c_{s2}\dot{d}_g(t) \tag{11}$$

in which: m_1 and m_2 are the payload masses; F_{f1} and F_{f2} are the friction forces of isolator bearings; μ is the damper friction coefficient; N_1 and N_2 are the variable damper normal forces exerted by the actuators; k_1 and k_2 are the isolator spring stiffness coefficients; m_{s1} and m_{s2} are equivalent lumped masses that represent the appendages distributed masses and accessories of the isolators; c_{s1}, c_{s2} and k_{s1}, k_{s2} are the inherent damping coefficients and the overall stiffness coefficients of the appendages, respectively; and sign$(\cdot)$ is the standard sign function. The excitation source is given by the displacement $d_g(t)$ imposed by the shaking-table and the corresponding velocity $\dot{d}_g(t)$.

The system parameters were experimentally determined. Those that are invariant for all the studied cases are: $m_{s1} = m_{s2} = 5.5$ kg, $k_{s1} = 2050$ N m^{-1}, $k_{s2} = 1.5k_{s1}$, $\xi_{s1} = 0.066$, $\xi_{s2} = 0.038$, $m_1 = m_2 = 7.73$ kg, $F_{f1} = 2.5$ N, $F_{f2} = 3.2$ N, and $\mu 0.5$. The rest of the parameters for each isolation alternative are displayed in Table 1.

The natural frequencies of the uncontrolled appendages with their respective payloads (original state) are $f_{s1} = 1.98$ Hz and $f_{s2} = 3.43$ Hz. The stiffness coefficients of each passive isolator are $k_1 = k_2 = 500$ N m^{-1}28 *are equal for all the studied cases sesook–body effectiveness must be assessed through simulations and/or experiments.test*. Consequently, the natural frequencies of the passively-isolated subsystems are $f_{\text{pis1}} \approx f_{\text{pis2}} \approx 1.3$ *Hz*. Thus, the necessary condition (5) of Section 2.2 ($\Delta_f \approx 0$) leads to the six feasible control alternatives summarized in Table 1: three of them use the *indirect* control method (2P, 2GH, 2SH); other three use the *direct* control method (2BHB, 1BHB_1P, 1NC_1BHB); and the uncontrolled case (2NC) is considered as a baseline for comparison. The trivial case 1NC_1P with an ideally-tuned passive isolator in which $f_{s1} \approx f_{\text{pis2}}$ was omitted because numerical simulations showed it leads to a slight improvement over the case 2NC, so a small detuning would make it underperforming in practice.

When using semi-active control, normal forces N_1 and N_2 are adjusted in real-time according to Eq. (7), which reduces to:

$$N_j = \begin{cases} N_{\max}, & \dot{x}_{Cj}(\dot{d}_j - \dot{d}_{sj}) > 0 \\ N_{\min}, & \dot{x}_{Cj}(\dot{d}_j - \dot{d}_{sj}) \leqslant 0 \end{cases}, \tag{12}$$

where: $j = 1, 2$ is the appendage number, $\mu N_{\max} = 10$ N and $\mu N_{\min} = 0$ N are the maximum and minimum damper forces, and $\dot{x}_{Cj}$ is defined according to Table 1.

Since the aim of this research is to evaluate the performance of different control isolation systems, two records lasting $T = 200$ s each, whose acceleration spectra are constant in the range 0.5–3 Hz, were used as excitation: a random Gaussian White Noise (WN) and a sine linear Frequency Sweep (FS). WN is the most general type of excitation while FS excitation was included in the study because it allows to assess the worst scenario (system at resonance) as in the case of car suspensions subjected to particular combinations of speeds and road wavelengths [38], satellites using Reaction Wheel Assemblies which can rotate in either direction [16] and structures excited by variable-speed rotating machinery.

Table 1
Isolation alternatives.

Case description	Case name	k_1	k_2	μN_1	μN_2	$\dot{x}_{C1}$	$\dot{x}_{C2}$
None of the appendages have isolation	2NC	10^5	10^5	10	10	–	–
Both appendages have passive isolation	2P	500	500	0	0	–	–
Both appendages have semi-active isolation using ground-hook	2GH	500	500	0–10	0–10	$\dot{d}_1 - \dot{d}_g$	$\dot{d}_2 - \dot{d}_g$
Both appendages have semi-active isolation using sky-hook	2SH	500	500	0–10	0–10	$\dot{d}_1$	$\dot{d}_2$
Both appendages have semi-active isolation using body-hook-body	2BHB	500	500	0–10	0–10	$\dot{d}_1 - \dot{d}_2$	$\dot{d}_2 - \dot{d}_1$
Appendage 1 has semi-active isolation using body-hook-body and appendage 2 has passive isolation	1BHB_1P	500	500	0–10	0	$\dot{d}_1 - \dot{d}_2$	–
Appendage 1 has no control and appendage 2 has semi-active isolation using body-hook-body	1NC_1BHB	10^5	500	10	0–10	–	$\dot{d}_2 - \dot{d}_1$

*SI units.

In order to use the same excitation on both, numerical and experimental models, the record measured by the laser sensor on the shaking table (Fig. 3) was used as displacement time history for loading the numerical model, i.e. $d_g(t)$ in Eqs. (8)-(11).

6. Results and discussion

The seven cases defined in Table 1 were experimentally tested by means of the setup shown in Fig. 3 using both excitation records and numerically simulated from Eqs. (8)–(12). Simulated results should be interpreted as the response of an ideal physical implementation because imperfections such as time delays, modal spillover and construction tolerances were assumed to have a negligible effect and therefore they were not taken into account in the numerical model. On the other hand, experimental results show the actual performance achieved in practice. Hence, the numerical model has been kept as simple as possible to capture the essential behaviour the proposed method to reduce relative vibrations in contrast to existing alternatives.

For the sake of clarity and briefness, system responses under FS are shown in frequency-domain (based on the whole 200 s response) while responses under WN excitation are shown in time-domain for a reduced time interval of 10 s only.

6.1. Case 2NC

For the uncontrolled case (2NC), Fig. 5(a, b) shows that the numerical model, in spite of its simplicity, acceptably matches the experimental results for both excitation records.

Fig. 5(b) displays that the relative displacement is large (yellow curve), when compared with individual displacements, due to two reasons: individual displacements amplitudes are large and the instantaneous phases are non-coincident most of the time because of the difference between frequencies, i.e. $f_1 = f_{s1} = 1.98$ Hz$\neq f_2 = f_{s2} = 2.43$ Hz $(\frac{2|\Delta_f|}{\Sigma_f} = 20\%)$. This is the main cause of poor performance, concerning relative vibration of the uncontrolled case, i.e. differences between dynamical properties of appendages.

6.2. Case 2P

Fig. 6(a) demonstrates that the incorporation of passive isolators (2P, *indirect* control method) drastically reduces the individual and relative displacements in the frequency range where the uncontrolled systems exhibit resonance (above 1.5 Hz). However, resonances are shifted to lower frequencies ($f_1 = f_{pis1} = 1.15$ Hz $< f_{s1}$, $f_2 = f_{pis2} = 1.27$ Hz $< f_{s2}$). As a result, the effectiveness of the *indirect* control method for controlling relative displacement is poor in low frequencies as in any isolation system. The ineffectiveness is mainly because the necessary condition (6) of Section 2.2 ($\Delta_A 0$) is not satisfied in low frequencies (yellow curves in Fig. 6(a)). This is problematic only if the actual excitation has significant frequency content in that band; for example, in satellites using Reaction Wheel Assemblies which can rotate in either direction.

As can be seen in Fig. 6(b), individual displacements are more correlated than in the previous case (Fig. 5(b)); which is because the natural frequencies are closer to each other $(\frac{2|\Delta_f|}{\Sigma_f} = 10\%)$ and, consequently, the relative-displacement amplitude is reduced (see yellow curves in Fig. 6(b)).

6.3. Case 2GH

For the case of using ground-hook control law in both appendages (2GH, *indirect* control method), Fig. 7(a) evidences the well-known benefit of adding semi-active control to isolation systems: individual displacements are controlled through the whole frequency range [18]. Fig. 7(b) shows that relative displacement is drastically reduced mainly because individual vibrations are low, despite differences in amplitudes and instantaneous phases. Thus, this is a trivial realization of the *indirect* control method.

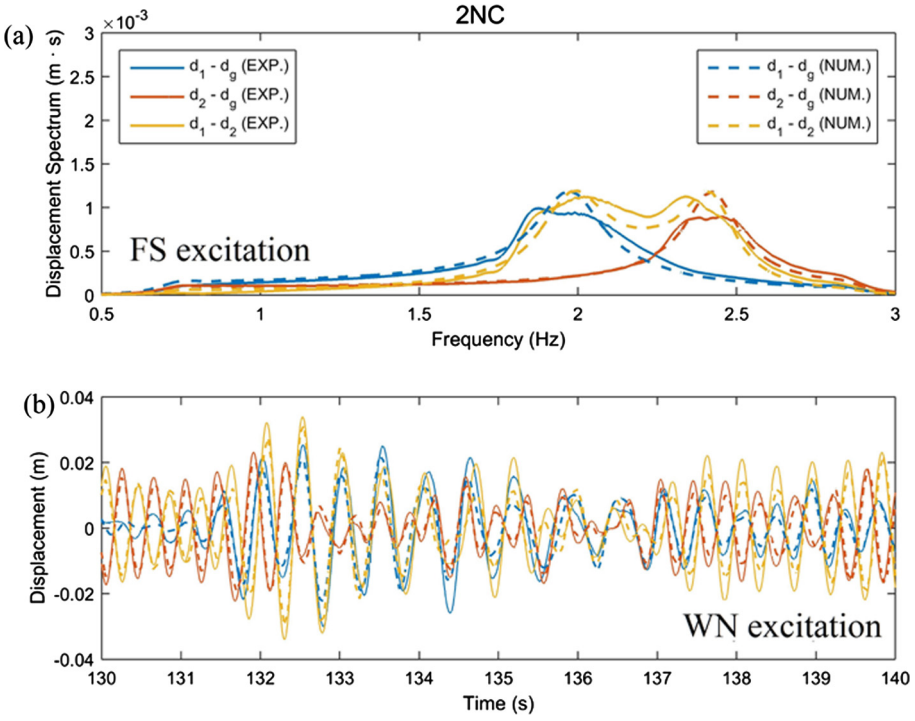

Fig. 5. Case 2NC, individual and relative displacements: (a) response in frequency-domain for Frequency-Sweep excitation, (b) response in time-domain for White-Noise excitation.

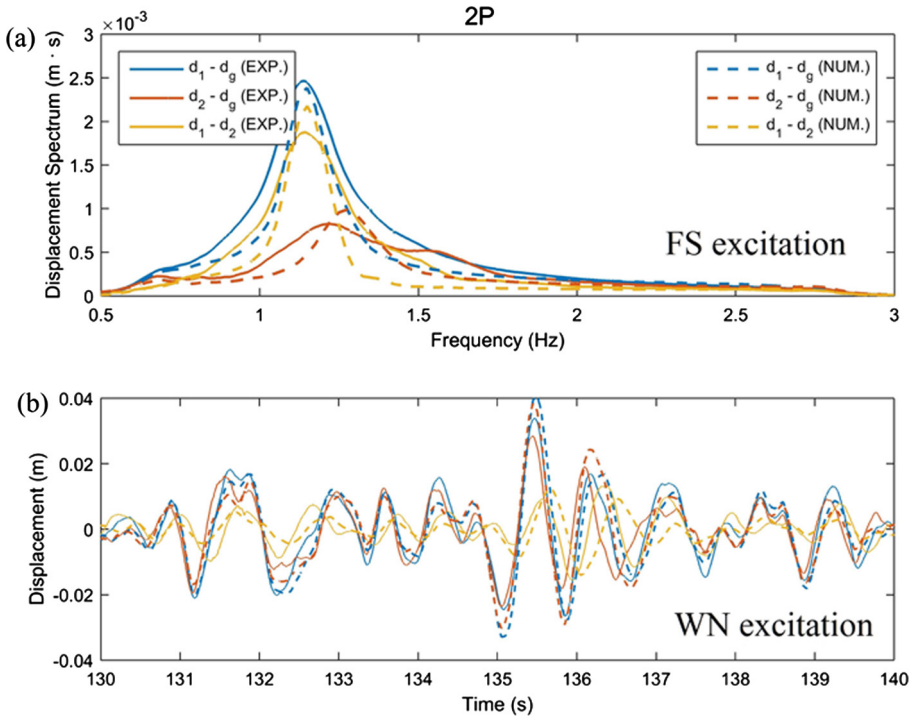

Fig. 6. Case 2P, individual and relative displacements: (a) response in frequency-domain for Frequency-Sweep excitation, (b) response in time-domain for White-Noise excitation.

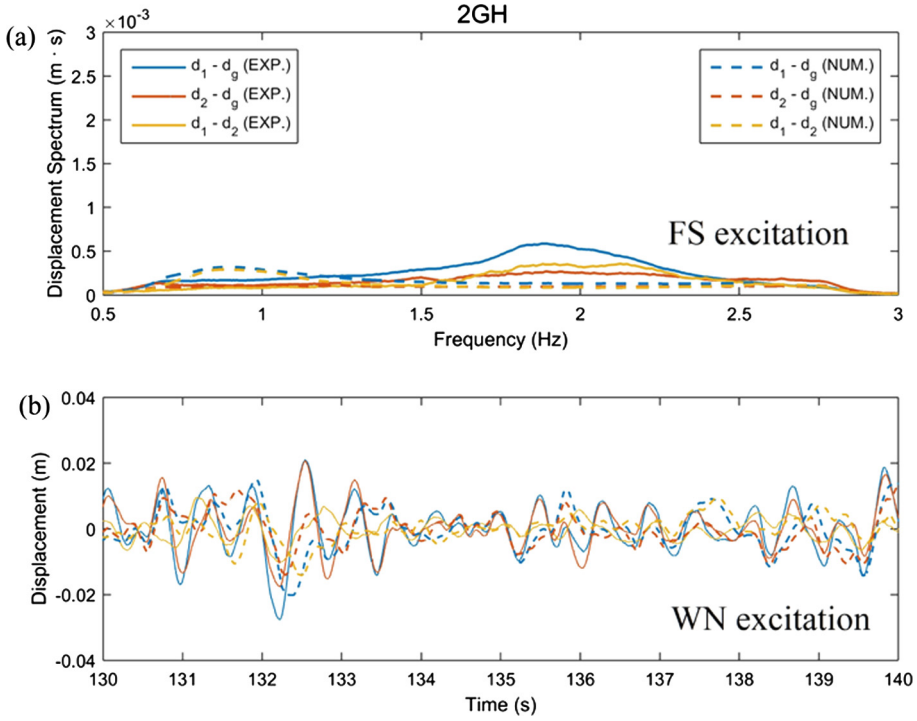

Fig. 7. Case 2GH, individual and relative displacements: (a) response in frequency-domain for Frequency-Sweep excitation, (b) response in time-domain for White-Noise excitation.

The main cause of mismatching between the experimental and numerical results of Fig. 7(a) is attributed to construction inaccuracies, which were not considered in order to keep the model as simple as possible.

6.4. Case 2SH

For the case of isolators semi-actively controlled by the sky-hook control law (2SH, *indirect* control method), Fig. 8(a) and (b)

show that individual and relative displacements are also controlled through the whole frequency range. As in the previous case, experimental results show a marginally lower reduction than simulated results, also attributed to construction inaccuracies.

A noticeably fact is that sky-hook, whose control objective is $\min|d_j|$, is as effective in reducing $d_j - d_g$ as ground-hook, whose control objective is $\min|d_j - d_g|$. This has been previously observed in vehicle suspension systems [33], where sky-hook, which is comfort-oriented, has a similar road-holding performance to that of ground-hook, which is road-holding oriented.

6.5. Case 2BHB

In this case, the two isolators are semi-actively controlled by the body-hook-body control law (2BHB, *direct* control method). In simple words, it is an implementation in which both payloads attempt to follow each other.

Assuming the isolators can be fully released or blocked, frequency f_1 can be semi-actively adjusted between $f_{min1} \approx f_{pis1} = 1.15$ Hz and $f_{max1} \approx f_{s1} = 1.98$ Hz, whereas f_2 can be adjusted between $f_{min2} \approx f_{pis2} = 1.27$ Hz and $f_{max2} \approx f_{s2} = 2.43$ Hz. Since $[f_{min1}, f_{max1}] \cap [f_{min2}, f_{max2}] = [1.27\text{ Hz}, 1.98\text{ Hz}] \neq \varnothing$, the necessary condition (5) of Section 2.2 ($\Delta_f \approx 0$) can be satisfied; i.e., control through the *direct* control method is feasible. Moreover, it is expected that $f_1 \cong f_2 \in [1.27\text{ Hz}, 1.98\text{ Hz}]$.

Fig. 9(a) shows that the simulated responses display coincident resonances at approximately 1.28 Hz ($\frac{2|\Delta_f|}{\Sigma_f} \approx 0$), while in the experimental ones, resonances are not so clear. Although experimental performance of 2BHB lightly differs from the simulated in the frequency range [1.27 Hz,1.98 Hz]; particularly around 1.5 Hz, it can be seen a slight local maxima of individual-displacement spectra (red and blue curves in Fig. 9(a)), both coincident with a local minimum of relative-displacement spectrum (yellow curve in Fig. 9(a)).

As shown in Fig. 9(b) for random vibration, the body-hook-body control law makes both individual displacements practically coincident in simulated responses while in the experimental ones, are only similar to each other.

6.6. Case 1BHB_1P

Fig. 10(a, b) shows the responses of the system with an implementation simpler than the previous one, in which one isolator is semi-actively controlled by the body-hook-body control law and the other one is passive (1BHB_1P, *direct* control method). In this case, the semi-actively controlled payload 1 attempts to follow the passively-isolated payload 2.

Assuming the semi-active isolator can be fully released or blocked, natural frequency f_1 can be adjusted between $f_{min1} \approx f_{pis1} = 1.15$ Hz and $f_{max1} \approx f_{s1} = 1.98$ Hz; whereas, natural frequency f_2 is constant and equal to $f_{pis2} = 1.27$ Hz. Since $f_{pis2} \in [f_{min1}, f_{max1}]$, necessary condition (5) of Section 2.2 ($\Delta_f \approx 0$) can be satisfied, and therefore, this *direct* control method is feasible. Moreover, it is expected that $f_1 \approx f_{pis2}$.

As can be seen in Fig. 10(a), semi-active control makes individual-displacement spectra (numerical and experimental) of payload 1 deform from light blue curves (payload 1 of case 2P) to adopt the shape of those of passively-isolated payload 2 (red curves) between 1 and 1.7 Hz ($\frac{2|\Delta_f|}{\Sigma_f} \approx 0$).

As regards to random vibration, Fig. 10(b) shows that the relative displacement is drastically reduced despite individual displacements remain large. This is because the three necessary conditions stated in Section 2.2 (i.e., $\Delta_0 \approx 0$, $\Delta_f \approx 0$ and $\Delta_A \approx 0$) tend to be fulfilled.

The numerical approximation of this case is better than that of 2GH, 2SH and 2BHB because the individual displacements are larger so mechanical imperfections are less significant.

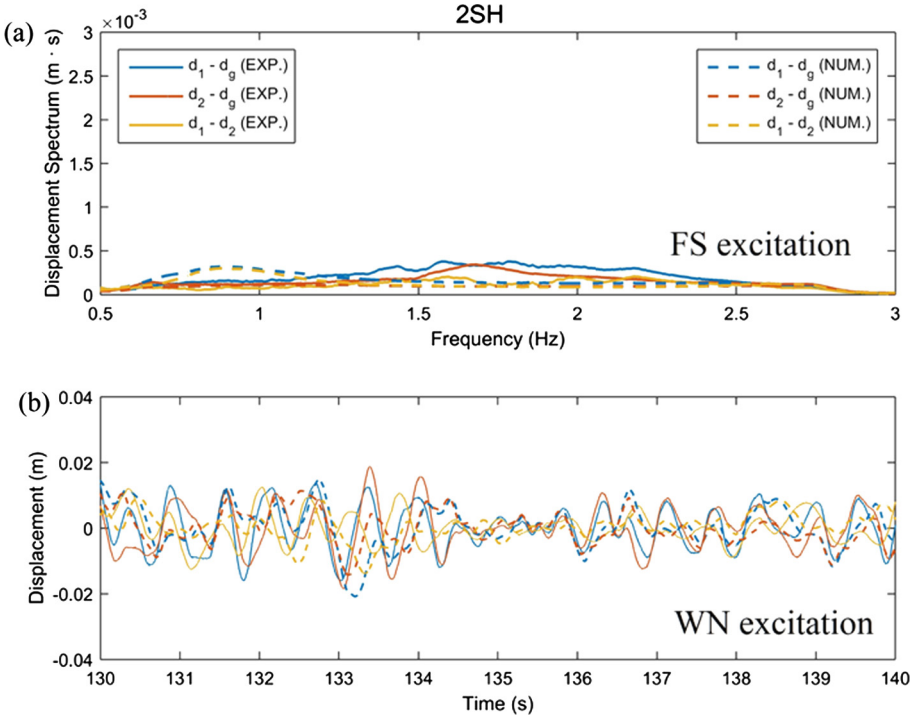

Fig. 8. Case 2SH, individual and relative displacements: (a) response in frequency-domain for Frequency-Sweep excitation, (b) response in time-domain for White-Noise excitation.

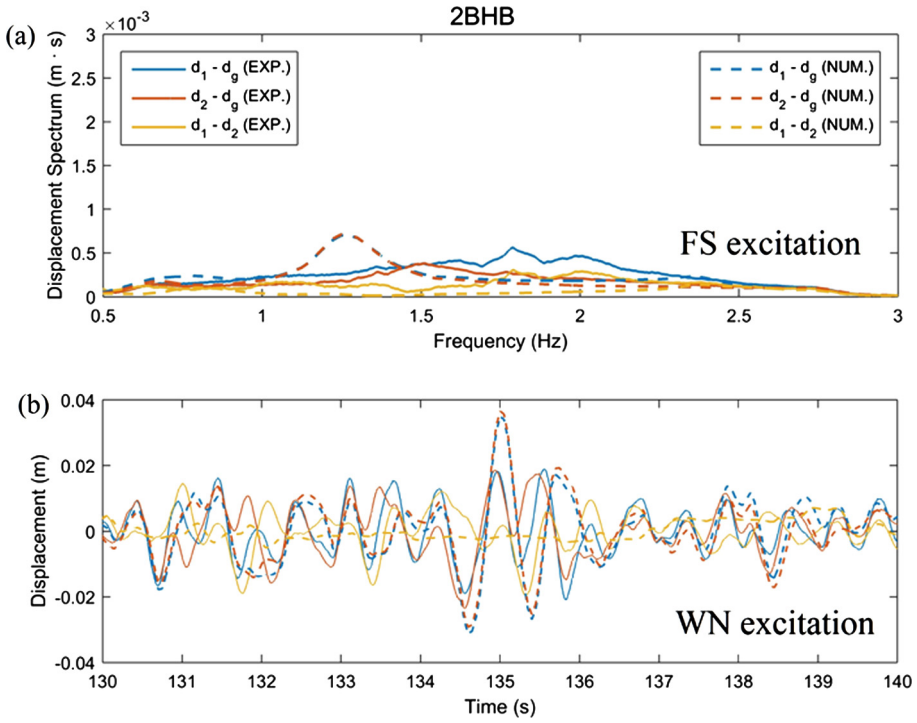

Fig. 9. Case 2BHB, individual and relative displacements: (a) response in frequency-domain for Frequency-Sweep excitation, (b) response in time-domain for White-Noise excitation.

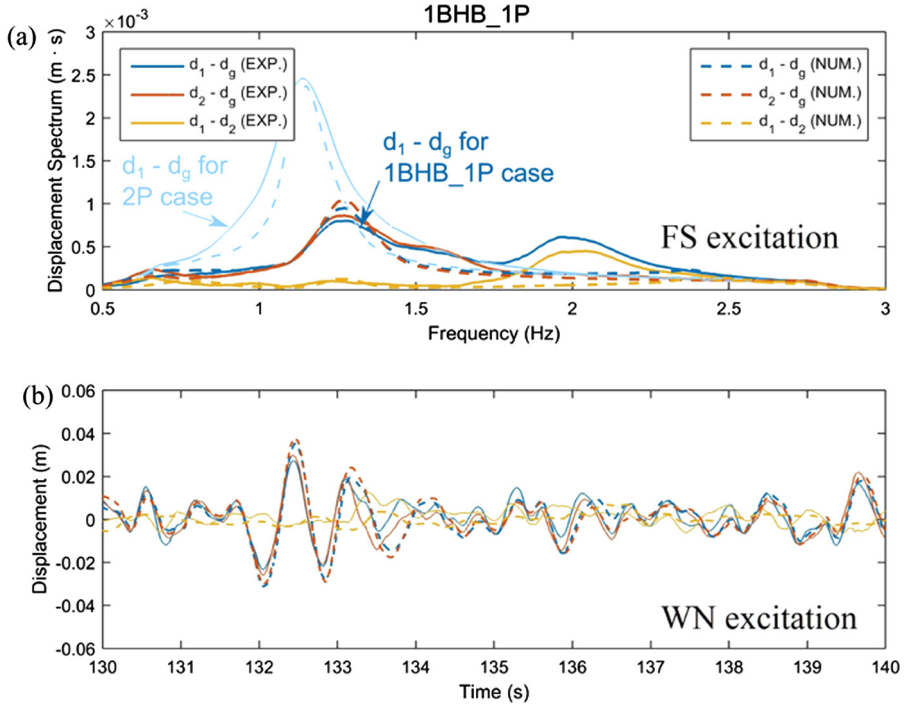

Fig. 10. Case 1BHB_1P, individual and relative displacements: (a) response in frequency-domain for Frequency-Sweep excitation, (b) response in time-domain for White-Noise excitation.

6.7. Case 1NC_BHB

Fig. 11(a) and (b) show the responses of the system in which the appendage 1 has no isolator and the appendage 2 has a semi-active isolator, also under the body-hook-body control law (1NC_BHB, *direct* control method). Thus, payload 2 attempts to follow non-isolated payload 1.

Assuming the same as in the cases 2BHB and 1BHB_1P, natural frequency f_2 can be adjusted between $f_{\min 2} \approx f_{\text{pis}2} = 1.27$ Hz and $f_{\max 2} f_{s2} = 2.43$ Hz, whereas natural frequency f_1 remains constant and equal to $f_{s1} = 1.98$ Hz. Hence, necessary condition (5) of Section 2.2 ($\Delta_f \approx 0$) can be satisfied since $f_{s1} \in [f_{\min 2}, f_{\max 2}]$ and therefore, this direct control method is feasible. Moreover, it is expected that $f_2 \approx f_{s1} = 1.98$ Hz.

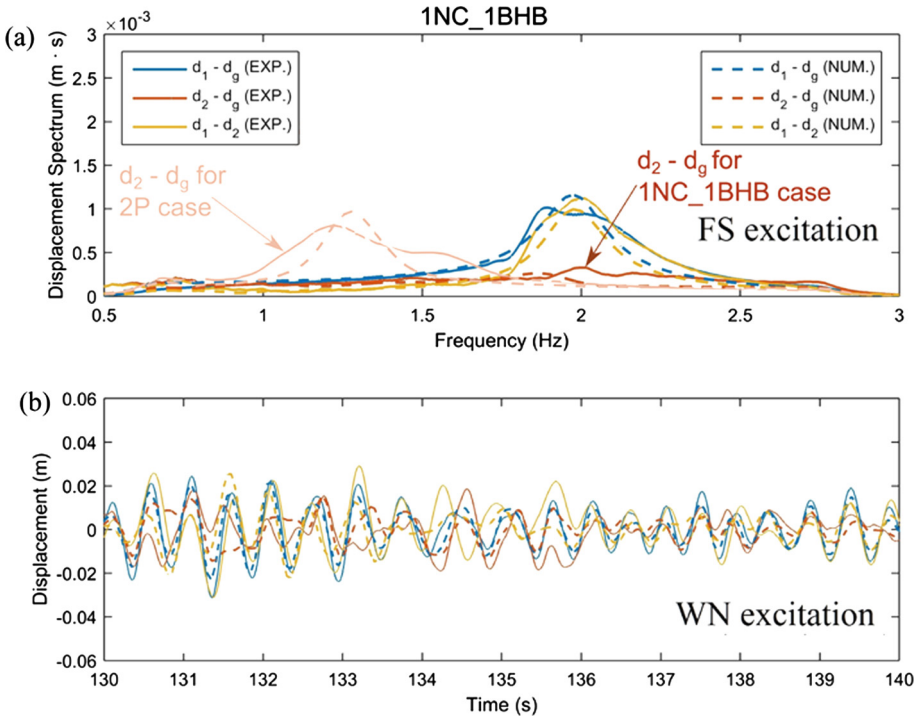

Fig. 11. Case 1NC_1BHB, individual and relative displacements: (a) response in frequency-domain for Frequency-Sweep excitation, (b) response in time-domain for White-Noise excitation.

As shown in Fig. 11(a), individual-displacement spectra of semi-actively-controlled payload 2 deform (from the passively-isolated payload 2, light red curves) to adopt the shape of those of uncontrolled payload 1 (blue curves, $f_{s1} = 1.98$ Hz). In this case, body-hook-body is effective in matching resonant frequencies ($\frac{2|\Delta_f|}{\Sigma_f} \approx 0$), as expected. However, the large change of frequency (from 1.27 Hz to 1.98 Hz) also leads to an important relative vibration reduction, though only partially in this case.

Summarizing, while necessary condition (5) of Section 2.2 ($\Delta_f \approx 0$) is satisfied (good correlation between individual displacements), as can be seen from Fig. 11(b), condition (6) ($\Delta_A \approx 0$) is not (individual displacements have different amplitudes).

7. Cost-effectiveness comparison

In order to quantify the effectiveness of each control alternative, two performance indices denoted by $J_{DIS\ peak}$ (normalized peak relative-displacement under FS excitation), and $J_{DIS\ RMS}$ (normalized root-mean-square (RMS) relative-displacement under WN excitation) are defined as follows:

$$J_{DIS\ peak} = \frac{\max_{0<t<T}|d_r(t)|}{\max_{0<t<T}|d_r^*(t)|} \tag{13}$$

$$J_{DIS\ RMS} = \sqrt{\frac{\int_0^T |d_r(t)|^2 dt}{\int_0^T |d_r^*(t)|^2 dt}} \tag{14}$$

where $d_r(t)$ and $d_r^*(t)$ are the relative displacements for the controlled and uncontrolled cases, respectively.

These performance indices are selected because peak value captures the worst scenario under FS excitation, while RMS value characterizes the average behaviour under WN excitation. Certainly, some applications are more sensitive to relative velocities than to relative displacements (e.g., motion blur in images [4]). In this regard, velocity-based performance indices were also evaluated. However, similar trends to $J_{DIS\ peak}$ and $J_{DIS\ RMS}$ were observed, so they are not displayed.

Fig. 12(a) shows the performance index, $J_{DIS\ peak}$, for all cases studied under FS excitation. It can be seen that case 2P underperformed the uncontrolled case, which is due to the resonance of isolation system at low frequencies. In the remaining cases, which displayed improvement over the uncontrolled case, the performance in numerically simulated cases was better than the experimental ones, because of construction inaccuracies as mentioned. In general, all the semi-active cases, excluding 1NC_1BHB, have similar performance: relative vibration is reduced to less than a half.

Under WN excitation, Fig. 12(b) shows that all the cases have lower RMS relative-displacement than the uncontrolled case (2NC); being the 1NC_1BHB the least effective. Moreover, case 2P was almost as effective as any of the semi-active cases.

Because of the small differences among the best cases (<20%), it is proposed to improve the assessment of the effectiveness of each control alternative by including the cost and complexity of each of them following an approach similar to that used in [33].

Costs were estimated, in relative terms, from the experience gained in the development of the experimental setup. Thus, arbitrarily choosing a relative cost C of a passive isolator as 1 (without loss of generality) and on the assumption that a semi-active isolator costs twice as much as a passive isolator does, since converting a passive isolator into a semi-active one is approximately as costly as implementing the original passive isolator, the seven studied cases have the following relative costs: $C(2NC) = 0$, $C(2P) = 2$, $C(2GH) = 4$, $C(2SH) = 4$, $C(2BHB) = 4$, $C(1BHB\_1P) = 3$, and $C(1NC\_1BHB) = 2$.

Evidently, as effectiveness is always desirable in a control system, the following two cost-effectiveness ratios are defined only for the useful cases (indices $J_{DIS\ peak}$ or $J_{DIS\ RMS}$ lower than 1):

$$r_{DIS\ peak} = \frac{C}{1 - J_{DIS\ peak}}, \quad J_{DIS\ peak} < 1, \tag{15}$$

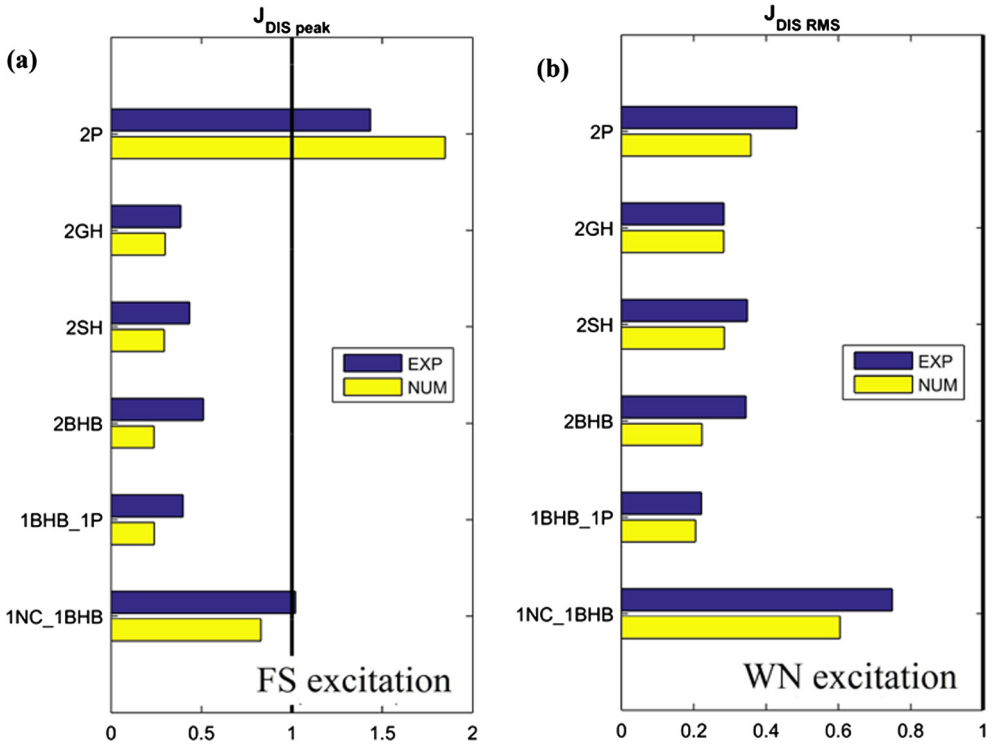

Fig. 12. Performance indices for the different studied cases under: (a) Frequency Sweep and (b) White Noise excitation.

$$r_{\text{DIS RMS}} = \frac{C}{1 - J_{\text{DIS RMS}}}, \quad J_{\text{DIS RMS}} < 1, \tag{16}$$

Cost-effectiveness ratios obtained from simulations and experiments are displayed in Table 2. To organize the information and summarize it, cost-effectiveness ratios in cells of each column were classified by k-means clustering analysis [39] into the following three groups (k = 3): 'economical', cells shaded in dark grey; 'intermediate', in light grey; and 'uneconomical' in white.

From simulated and experimental results, Table 2 displays that 2P is 'economical' under WN excitation, but it becomes 'uneconomical' under FS excitation. Conversely, from simulated results, the other *indirect* control method alternatives using semi-active control (2GH and 2SH) are 'economical' for FS excitation but they become 'uneconomical' for WN excitation because case 2P has similar performance but at lower cost. Cases 2BHB and 1NC_1BHB, which are based on the *direct* control method, are 'economical' or 'intermediate' in terms of both performance indices. For its part, the case 1NC_1P using an ideally-tuned isolator (studied only numerically, not shown) displayed $J_{\text{DIS peak}} = 0.8$ and $r_{\text{DIS peak}} = 5.1$, so it would be 'economical' in ideal conditions though not as much as 1BHB_1P. Finally, it can be concluded that 1BHB_1P is 'economical' in terms of both performance indices as it was confirmed by the numerical and experimental assessment. Therefore, 1BHB_1P is the best of the studied control alternatives when costs and different excitation types are considered.

Despite costs assigned are true for this testbed, values can vary in actual implementations. Nevertheless, the main conclusion of

Table 2
Cost-effectiveness comparison.

		Cost-effectiveness ratios based on simulations (achievable performances)		Cost-effectiveness ratios based on experiments (achieved performances)	
Method	Case name	$r_{\text{DIS peak}}$ (FS excitation)	$r_{\text{DIS RMS}}$ (WN excitation)	$r_{\text{DIS peak}}$ (FS excitation)	$r_{\text{DIS RMS}}$ (WN excitation)
Indirect	2P	-*	3.12	-*	3.88
"	2GH	5.71	5.58	6.51	5.58
"	2SH	5.66	5.59	7.08	6.13
Direct	2BHB	5.24	5.15	8.17	6.10
"	1BHB_1P	3.94	3.77	4.99	3.85
"	1NC_1BHB	11.70	5.06	-	7.96
Reference for shading: 'economical' in dark grey, 'intermediate' in light grey, and 'uneconomical' in white.					

Reference for shading: 'economical' in dark grey, 'intermediate' in light grey, and 'uneconomical' in white.
*Not evaluated, $J_{\text{DIS peak}} > 1$, see Fig. 12.

this work remains qualitatively true even if different, but realistic, costs are assumed, and both excitation types are considered. This is because, as shown in Fig. 12(a), the only competitors for 1BHB_1P are 2GH, 2SH and 2BHB but with higher cost.

8. Conclusions

For the problem of controlling relative vibrations between two subsystems, two control methods based on passive and semi-active isolation systems are presented: the *indirect* control method (classical), which seeks to control the relative vibrations through the reduction of individual vibrations; and the *direct* control method (proposed), which is based on the reduction of relative motion. Moreover, three necessary conditions were found to assess the feasibility of implementing this last method: individual displacements must have the same offset phases, frequencies, and amplitudes. Violations of the first two conditions can be easily identified a priori, thereby reducing the universe of possible design configurations. A control law called body-hook-body, obtained from the generalization of traditional ground-hook and sky-hook control laws, was proposed for the semi-active isolation system classified as *direct* control method.

In order to explore the capabilities and limitations of different methods for controlling relative vibrations, 7 cases that combine passive and semi-active isolators were numerically and experimentally studied: 3 control alternatives implementing the *indirect* control method, 3 control alternatives implementing the *direct* control method, and the uncontrolled case for reference.

The main conclusion of this work is that the proposed 1BHB_1P implementation (*direct* control method scheme) which uses a passive isolator and a semi-active isolator is slightly more effective than the traditional *indirect* control methods (2GH or 2SH), but with three-fourths the cost of them; which means a 30% reduction of cost-effectiveness ratio.

The particular behaviour in frequency-domain of this configuration is that the semi-actively-isolated subsystem finely tunes their properties attempting to imitate the motion of the other passively-isolated subsystem resulting in two subsystems with similar spectral characteristics.

Acknowledgements

The authors would like to thank National Research Council from Argentina (CONICET) and National University of Cuyo for the financial support. The helps received from Eng. Gabriel Houri, during the preparation and execution of the experiments, and from Public Translator Cinthia Garrido, in the English proofread of this paper, is also gratefully acknowledged.

Appendix A

When comparing sine functions with different but close offset phases, their absolute difference ($|\Delta_\theta|$) can be considered as an estimate measure of the closeness between them. This is a representative figure because the normalized correlation between sine functions having the same amplitude and frequency but different offset phases equals $\cos(\Delta_\theta)$, which is monotonically decreasing with $|\Delta_\theta|$ if $|\Delta_\theta| \leqslant \pi$ rad.

Similarly, if frequencies are close but different, their absolute difference normalized with respect to their average $\left(\frac{2|\Delta_f|}{\Sigma_f}\right)$ can be considered as an estimate measure of the frequency closeness. This is a representative figure because, as shown below, the normalized correlation between sine functions having the same amplitude and phase but different frequency is monotonically decreasing with $\frac{2|\Delta_f|}{\Sigma_f}$ if $\frac{2|\Delta_f|}{\Sigma_f} \leqslant 50\%$.The normalized correlation between sine signals with different frequency strongly depends on the particular time period chosen for the evaluation. This is because the frequency difference leads to a time lag that increases with time and then decreases. However, if signals are forced responses of vibrating systems under correlated excitation, correlation must be evaluated in a short time because the excitation drives them to be in phase.

Consider two sine signals having the same amplitude and offset phase ($\theta_1 = \theta_2 = 0$ rad, without loss of generality) but different frequencies, namely:

$$x_1(t) = \sin(2\pi f_1 t) \tag{A.1}$$

$$x_2(t) = \sin(2\pi f_2 t) \tag{A.2}$$

Their normalized correlation in a time period equal to the average period is calculated as:

$$c_N = \frac{1}{\|x_1(t)\|\|x_2(t)\|}\langle x_1(t), x_2(t)\rangle \tag{A.3}$$

where $\cdot,\cdot$ is the truncated inner product between continuous functions on the interval $\left[0, \left(\frac{\Sigma_f}{2}\right)^{-1}\right]$ and $\|\cdot\|$ is the norm induced by that inner product. On one hand:

$$\begin{aligned}\langle x_1(t), x_2(t)\rangle &= \int_0^{\left(\frac{\Sigma_f}{2}\right)^{-1}} \sin(2\pi f_1 t)\sin(2\pi f_2 t)dt \\ &= \frac{1}{2\pi 2\Delta_f}\sin\left(2\pi\frac{2\Delta_f}{\Sigma_f}\right)\end{aligned} \tag{A.4}$$

On the other hand:

$$\|x_1(t)\|^2 = \langle x_1(t), x_1(t)\rangle = \int_0^{f_1^{-1}} \sin^2(2\pi f_1 t)dt = \frac{1}{2f_1}, \tag{A.5}$$

$$\|x_2(t)\|^2 = \frac{1}{2f_2} \tag{A.6}$$

and, therefore:

$$\frac{1}{\|x_1(t)\|\|x_2(t)\|} = 2\sqrt{f_1 f_2} \cong \Sigma_f \tag{A.7}$$

since the difference between arithmetic and geometric means is less than 6% when the difference between frequencies is less than 50%.

Then, combining Eqs. (A.3), (A.4) and (A.7) yields:

$$c_N = 2\sqrt{f_1 f_2}\frac{1}{2\pi 2\Delta_f}\sin\left(2\pi\frac{2\Delta_f}{\Sigma_f}\right)\frac{1}{2\pi\frac{2\Delta_f}{\Sigma_f}}\sin\left(2\pi\frac{2\Delta_f}{\Sigma_f}\right) \tag{A.8}$$

Besides, in the particular case in which $\Delta_f = 0$ it is trivial that $c_N = 1$ (perfect correlation). As a result, it can be stated that:

$$c_N \approx \mathrm{sinc}\left(2\pi\frac{2\Delta_f}{\Sigma_f}\right) \tag{A.9}$$

where $\mathrm{sinc}(\cdot)$ is the cardinal sine function, which is monotonically decreasing with $\frac{2|\Delta_f|}{\Sigma_f}$ if $\frac{2|\Delta_f|}{\Sigma_f} \leqslant 50\%$.

References

[1] Soong TT, Dargush GF. Passive energy dissipation systems in structural engineering. Chichester, UK: John Wiley & Sons; 1997.
[2] Garrido H, Curadelli O, Ambrosini D. Experimental and theoretical study of semi-active friction tendons. Mechatronics 2016;39:63–76. https://doi.org/10.1016/j.mechatronics.2016.08.005.
[3] Kelly R, Carelli R, Nasisi O, Kuchen B, Reyes F. Stable visual servoing of camera-in-hand robotic systems. IEEE/ASME Trans Mechatronics 2000;5:39–48. https://doi.org/10.1109/3516.828588.

[4] Stern A, Kopeika NS. General restoration filter for vibrated-image restoration. Appl Opt 1998;37:7596–603. https://doi.org/10.1364/AO.37.007596.
[5] Gran MH, Bronowicki AJ. Semi-active vibration isolator and fine positioning mount, US006022005A; 2000.
[6] Makihara K, Onoda J, Minesugi K. New approach to semi-active vibration isolation to improve the pointing performance of observation satellites. Smart Mater Struct 2006;15:342–50. https://doi.org/10.1088/0964-1726/15/2/014.
[7] Oh H-U, Choi Y-J. Enhancement of pointing performance by semi-active variable damping isolator with strategies for attenuating chattering effects. Sensors Actuators A Phys 2011;165:385–91. https://doi.org/10.1016/j.sna.2010.11.009.
[8] Wang W-C, Lee J-W, Chen K-S, Liu Y-H. Design and vibration control of a notch-based compliant stage for display panel inspection applications. J Sound Vib 2014;333:2701–18. https://doi.org/10.1016/j.jsv.2014.01.012.
[9] Caron B, Balik G, Brunetti L, Jeremie A. Vibration control of the beam of the future linear collider. Control Eng Pract 2012;20:236–47. https://doi.org/10.1016/j.conengprac.2011.11.001.
[10] Neat GW, Abramovici A, Goullioud R, Korechoff RP, Calvet RJ, Joshi SS. Overview of the microprecision interferometer testbed, Pasadena; 1998.
[11] Rivin EI. Vibration isolation of precision equipment. Precis Eng 1995;17:41–56. https://doi.org/10.1016/0141-6359(94)00006-L.
[12] Kim C-J, Oh J-S, Park C-H. Modelling vibration transmission in the mechanical and control system of a precision machine. CIRP Ann – Manuf Technol 2014;63:349–52. https://doi.org/10.1016/j.cirp.2014.03.133.
[13] Pratesi F, Sorace S, Terenzi G. Analysis and mitigation of seismic pounding of a slender R/C bell tower. Eng Struct 2014;71:23–34. https://doi.org/10.1016/j.engstruct.2014.04.006.
[14] Sharma K, Deng L, Noguez CC. Field investigation on the performance of building structures during the April 25, 2015, Gorkha earthquake in Nepal. Eng Struct 2015;121(2016):61–74. https://doi.org/10.1016/j.engstruct.2016.04.043.
[15] Paolacci F, Giannini R, De Angelis M. Seismic response mitigation of chemical plant components by passive control techniques. J Loss Prev Process Ind 2013;26:924–35. https://doi.org/10.1016/j.jlp.2013.03.003.
[16] Preumont A. Vibration control of active structures: an introduction. 3rd ed. Netherlands, Dordrecht: Springer; 2011. https://doi.org/10.1007/978-94-007-2033-6.
[17] Garrido H. Control semiactivo de vibraciones en sistemas estructurales. PhD thesis. Universidad Nacional de Cuyo; 2015.
[18] Casciati F, Magonette G, Marazzi F. Technology of semiactive devices and applications in vibration mitigation. Chichester, UK: John Wiley & Sons Ltd; 2006. https://doi.org/10.1002/0470022914.
[19] Bitaraf M, Ozbulut OE, Hurlebaus S, Barroso L. Application of semi-active control strategies for seismic protection of buildings with MR dampers. Eng Struct 2010;32:3040–7. https://doi.org/10.1016/j.engstruct.2010.05.023.
[20] Symans MD, Constantinou MC. Semi-active control systems for seismic protection of structures: a state-of-the-art review. Eng Struct 1999;21:469–87. https://doi.org/10.1016/S0141-0296(97)00225-3.
[21] Preumont A, Seto K. Active control of structures. Chichester, UK: John Wiley & Sons; 2008.
[22] Karnopp D, Crosby MJ, Harwood RA. Vibration control using semi-active force generators. ASME J Ind 1974;96:619–26.
[23] Makihara K, Onoda J, Tsuchihashi M. Investigation of performance in suppressing various vibrations with energy-recycling semi-active method. Acta Astronaut 2006;58:506–14. https://doi.org/10.1016/j.actaastro.2006.01.007.
[24] Gawronski W. Advanced structural dynamics and active control of structures. New York: Springer; 2004.
[25] Garrido H, Curadelli O, Ambrosini D. A straightforward method for tuning of Lyapunov-based controllers in semi-active vibration control applications. J Sound Vib 2014;333:1119–31.
[26] Garrido H, Curadelli O, Ambrosini D. Control semiactivo en la mitigación de vibraciones relativas de instrumentos soportados por subestructuras flexibles, en: Asociación Argentina de Tecnología Espacial (Ed.), VII Congr. Argentino Tecnol. Espac., Mendoza; 2013.
[27] Koo J-H, Shukla A, Ahmadian M. Dynamic performance analysis of non-linear tuned vibration absorbers. Commun Nonlinear Sci Numer Simul 2008;13:1929–37. https://doi.org/10.1016/j.cnsns.2007.03.020.
[28] Clough RW, Penzien J. Dynamics of structures. 3rd ed. Berkeley, CA 94704 USA: Computers & Structures Inc.; 1995.
[29] Soong TT, Spencer Jr BF. Supplemental energy dissipation: state-of-the-art and state-of-the-practice. Eng Struct 2002;24:243–59. https://doi.org/10.1016/S0141-0296(01)00092-X.
[30] Spelta C, Savaresi SM, Fabbri L. Experimental analysis of a motorcycle semi-active rear suspension. Control Eng Pract 2010;18:1239–50. https://doi.org/10.1016/j.conengprac.2010.02.006.
[31] Koo J-H. Using magneto-rheological dampers in semiactive tuned vibration absorbers to control structural vibrations. Virginia Polytechnic Institute and State University; 2003.
[32] Viet LD, Nghi NB, Hieu NN, Hung DT, Linh NN, Hung LX. On a combination of ground-hook controllers for semi-active tuned mass dampers. J Mech Sci Technol 2014;28:2059–64. https://doi.org/10.1007/s12206-014-0109-3.
[33] Savaresi SM, Poussot-Vassal C, Spelta C, Sename O, Dugard L. Semi-active suspension control design for vehicles. Amsterdam - Boston - Heidelberg - London - New York - Oxford Paris - San Diego - San Francisco - Singapore - Sydney - Tokyo: Elsevier; 2010.
[34] Balas MJ. Trends in large space structure control theory: Fondest hopes, wildest dreams. IEEE Trans Automat Contr 1982;27:522–35. https://doi.org/10.1109/TAC.1982.1102953.
[35] Azadi M, Fazelzadeh Sa, Eghtesad M, Azadi E. Vibration suppression and adaptive-robust control of a smart flexible satellite with three axes maneuvering. Acta Astronaut 2011;69:307–22. https://doi.org/10.1016/j.actaastro.2011.04.001.
[36] Gasbarri P, Monti R, Sabatini M. Very large space structures: non-linear control and robustness to structural uncertainties. Acta Astronaut 2014;93:252–65. https://doi.org/10.1016/j.actaastro.2013.07.022.
[37] Song G, Agrawal BN. Vibration suppression of flexible spacecraft during attitude control. Acta Astronaut 2001;49:73–83. https://doi.org/10.1016/S0094-5765(00)00163-6.
[38] Dixon JC. The shock absorber handbook. 2nd ed. The Atrium, Southern Gate, Chichester: John Wiley & Sons Ltd; 2007.
[39] Jain AK. Data clustering: 50 years beyond K-means. Pattern Recognit Lett 2010;31:651–66. https://doi.org/10.1016/j.patrec.2009.09.011.
[40] Garrido H, Curadelli O, Ambrosini D. Equivalencia entre sistemas de control de vibraciones pasivos y semiactivos, en: XX Congr. sobre Métodos Numéricos y sus Apl. – ENIEF 2013, Mecánica Computacional, vol. XXXII, Mendoza – Argentina; 2013. p. 2153–74.